Electronic Supporting Information

Metallic Cu_2N monolayer with planar tetracoordinated nitrogen as a promising catalyst for CO_2 electroreduction

Jingjing Jia,[a] Zhongxu Wang,[a] Yu Li,[b] Fengyu Li,[b,*] Yongchen Shang,[a] Yuejie Liu,[c,*] Qinghai Cai,[a,d] Jingxiang Zhao[a,*]

[a] *College of Chemistry and Chemical Engineering, and Key Laboratory of Photonic and Electronic Bandgap Materials, the Ministry of Education, Harbin Normal University, Harbin, 150025, China*

[b] *School of Physical Science and Technology, Inner Mongolia University, Hohhot, 010021, China*

[c] *Modern Experiment Center, Harbin Normal University, Harbin, 150025, China*

[d] *Heilongjiang Province Collaborative Innovation Center of Cold Region Ecological Safety, Harbin 150025, China*

[*] To whom correspondence should be addressed. Email: *fengyuli@imu.edu.cn* (FL); *zjx1103@hotmail.com* (YL) and *xjz_hmily@163.com* (JZ)

Computational Details on Free Energy Profiles and Dissolution Potential

On the basis of the CHE model, the ΔG value of each elementary step in the CO_2RR can be obtained by $\Delta G = \Delta E + \Delta E_{ZPE} - T\Delta S + \Delta G_{pH} + \Delta G_U$, where the reaction energy difference (ΔE) can be directly computed from DFT computations. ΔE_{ZPE} and ΔS are the changes in the zero-point energies and entropy between the products and the reactants at room temperature (T = 298.15 K), which can be calculated from the vibrational frequencies, while the entropies of the free molecules, including CO_2, CH_4, C_2H_4, CO and H_2, were taken from the NIST database. ΔG_{pH} is the free energy correction of pH, which can be calculated by $\Delta G_{pH} = k_B T \times pH \times \ln 10$, and the pH value was set to be zero in this work. $\Delta G_U = -eU$, where e is the transferred charge and U represents the applied potential at the electrode. The limiting potential (U_L) was used to evaluate the Cu_2N towards the CO_2RR, which will be obtained from the free energy change of the potential-determining step (ΔG_{PDS}) along the lowest energy pathway: $U_L = -\Delta G_{max}/e$, and a less negative U_L value denotes less energy input, thus suggesting better catalytic performance.

To evaluate the stability of Cu_2N monolayer in strong acidic media, we computed the dissolution potentials (U_{dis}, in V) of Cu in Cu_2N monolayer at pH = 0, which was defined as: $U_{dis} = U_{Cu}^{0} + \left[E_{Cu,bulk} - \left(E_{Cu_2N} - E_{d-Cu_2N}\right)\right]/ne$, where U_{Cu}^{0} is the standard dissolution potential of Cu in the bulk form (1.21 V), $d-Cu_2N$ is the defective Cu monolayer by dissolving (removing) one Cu to solutions, and *n* is the coefficient for the aqueous dissolution reaction: $Cu + 2H^+ \leftrightarrow Cu^{2+} + H_2$, namely, *n*

equals to 2. According to this definition, the U_{dis} value of Cu in Cu_2N monolayer is computed to be about 1.01 V.

Table S1. Elastic constants (C_{11}, C_{22}, C_{12}, C_{44}, in N m^{-1}) of the Cu_2N monolayer.

System	C_{11}	C_{22}	C_{12}	C_{44}
Cu_2N	114.72	114.72	46.69	1.87

Table S2. The computed free energy changes of each possible elementary step during the electrochemical reduction of CO to CH_4 and C_2H_4 on Cu_2N monolayer.

Elementary step	Free energy change (ΔG)
CO_2 (g)+ $H^+ + e^- \rightarrow {}^*COOH$	–0.03
CO_2 (g)+ $H^+ + e^- \rightarrow {}^*HCOO$	0.62
${}^*COOH + H^+ + e^- \rightarrow {}^*CO + H_2O$	0.12
${}^*CO \rightarrow CO + *$	0.93
${}^*COOH + H^+ + e^- \rightarrow {}^*HCOOH$	1.45
${}^*HCOH \rightarrow HCOH + *$	1.23
${}^*COOH + H^+ + e^- \rightarrow {}^*COHOH$	0.97
${}^*CO + H^+ + e^- \rightarrow {}^*HCO$	–0.12
${}^*CO + H^+ + e^- \rightarrow {}^*COH$	0.74
${}^*HCO + H^+ + e^- \rightarrow {}^*HCOH$	0.33
${}^*HCO + H^+ + e^- \rightarrow {}^*H_2CO$	1.14
${}^*HCOH + H^+ + e^- \rightarrow {}^*H_2COH$	–0.12
${}^*HCOH + H^+ + e^- \rightarrow {}^*CH + H_2O$	0.38
${}^*H_2COH + H^+ + e^- \rightarrow {}^*CH_2 + H_2O$	–0.32
${}^*H_2COH + H^+ + e^- \rightarrow {}^*H_3COH$	0.45
${}^*H_3COH \rightarrow H_3COH + *$	0.01
${}^*CH_2 + H^+ + e^- \rightarrow {}^*CH_3$	–0.53
${}^*CH_3 + H^+ + e^- \rightarrow CH_4 + {}^*$	–0.36
${}^*CH_2 + CO$ (g) + $e^- \rightarrow {}^*CH_2$-CO	–0.33

$^{*}CH_2–CO + H^+ + e^– \rightarrow {}^{*}CH_2–COH$	0.13
$^{*}CH_2–CO + H^+ + e^– \rightarrow {}^{*}CH_3–CO$	0.25
$^{*}CH_2–COH + H^+ + e^– \rightarrow {}^{*}CH_2–CHOH$	0.20
$^{*}CH_2–COH + H^+ + e^– \rightarrow {}^{*}CH_3–COH$	0.79
$^{*}CH_2–COH + H^+ + e^– \rightarrow {}^{*}CH_2–COH_2$	1.24
$^{*}CH_2–HCOH + H^+ + e^– \rightarrow {}^{*}CH_2–HC+H_2O$	–0.46
$^{*}CH_2–HCOH + H^+ + e^– \rightarrow {}^{*}CH_3–HCOH$	0.92
$^{*}CH_2–HCOH + H^+ + e^– \rightarrow {}^{*}CH_2–H_2COH$	0.58
$^{*}CH_2–HC + H^+ + e^- \rightarrow CH_2H_2 + *$	–0.41
$^{*}CH_2–HC + H^+ + e^– \rightarrow {}^{*}CH_3–HC$	0.23

Table S3. The computed free energy changes (ΔG in eV) of CO_2 to $COOH^*$ and magnetic moment (M in μ_B) of TM and N sites within TM_2N monolayers (TM = Mn, Fe, Ni, Cu) monolayer.

System	ΔG on TM site	ΔG on N site	M_{TM}	M_N
Mn_2N	–2.45	–1.79	2.78	–0.18
Fe_2N	–1.13	–0.54	2.07	–0.11
Ni_2N	+1.21	+0.76	0.00	0.00
Cu_2N	+1.45	–0.03	0.13	0.19

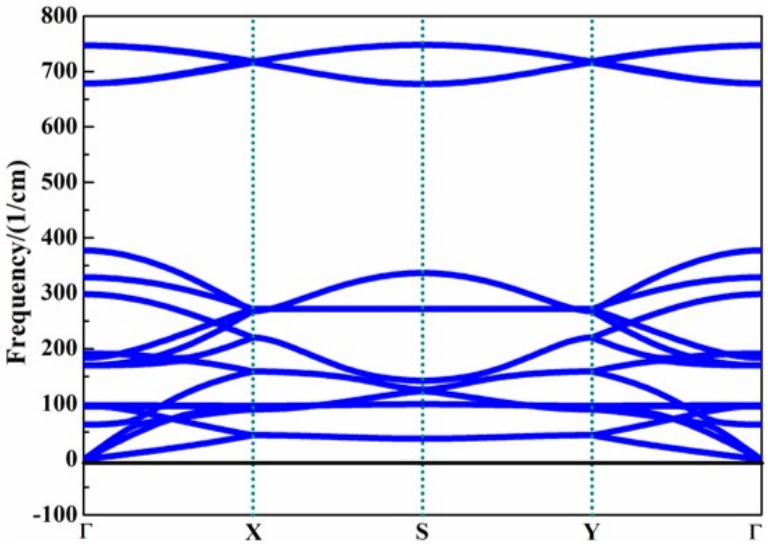

Fig. S1. The computed phonon dispersions of the predicted Cu_2N monolayer.

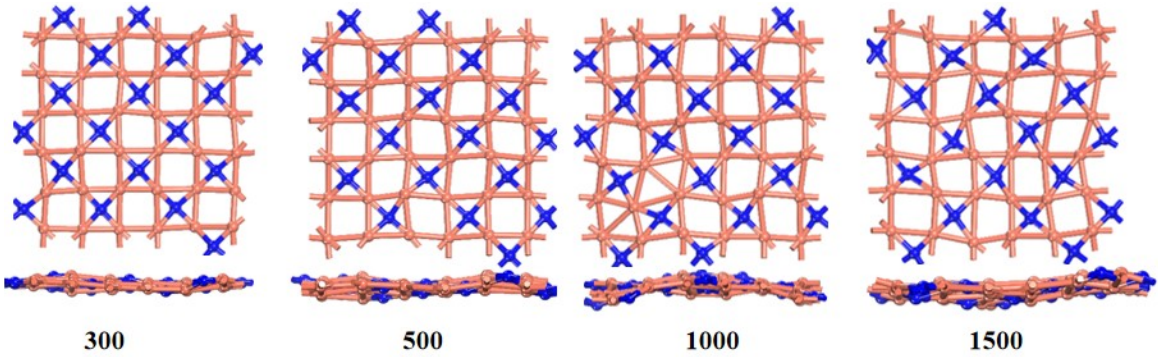

Fig. S2. Snapshots of Cu_2N equilibrium structures at varieties temperatures after 10 ps AIMD simulations.

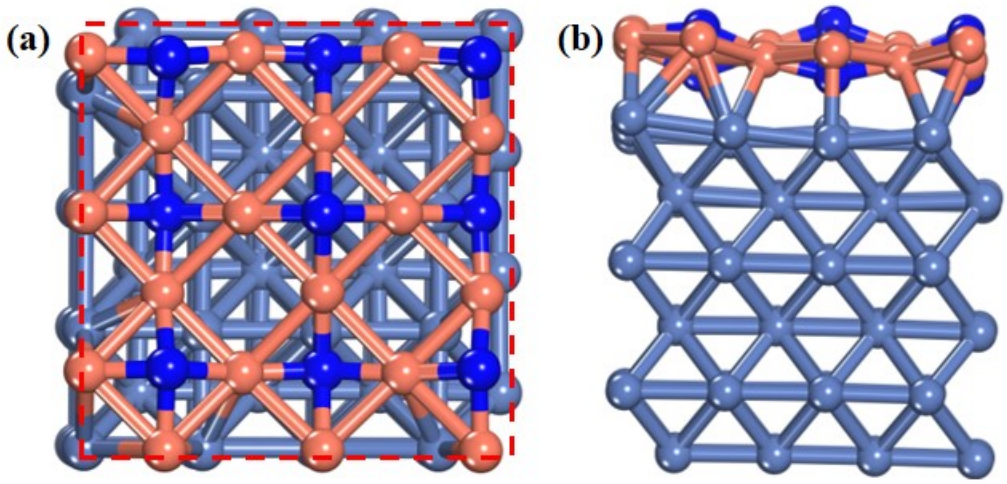

Fig. S3. (a) Top and (b) side views of the ball and stick model of the Cu_2N/Cu(100). Cu(100) and the Cu and N atoms of Cu_2N are denoted by blue gray, orange and blue spheres, respectively.

The formation energy (E_{form}) of Cu_2N monolayer on Cu(100) substrate was defined as: $E_{form} = E_{Cu_2N/Cu(100)} - N \times E_{Cu} - M \times E_N - E_{Cu(100)}$, where $E_{Cu_2N/Cu(100)}$ is the total energy of Cu_2N/Cu(100), N and M represent the number of Cu and N atoms in the Cu_2N monolayer, E_{Cu} and E_N can be computed from Cu bulk and N_2 gas, and $E_{Cu(100)}$ is the energy of Cu(100) substrate.

The cleavage energy (E_{cl}) of the exfoliation of Cu_2N monolayer from Cu(100) substrate was determined by:

$$E_{cl} = \frac{E_{Cu_2N} + E_{Cu(100)} - E_{Cu_2N/Cu(100)}}{A}$$

where E represents the electronic energies, where A is the interface area.

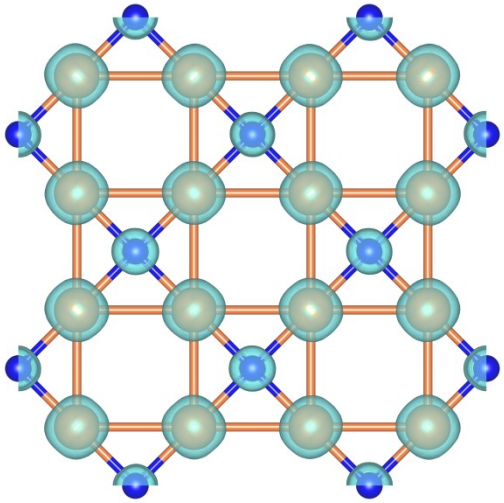

Fig. S4. Spin density of Cu_2N monolayer.

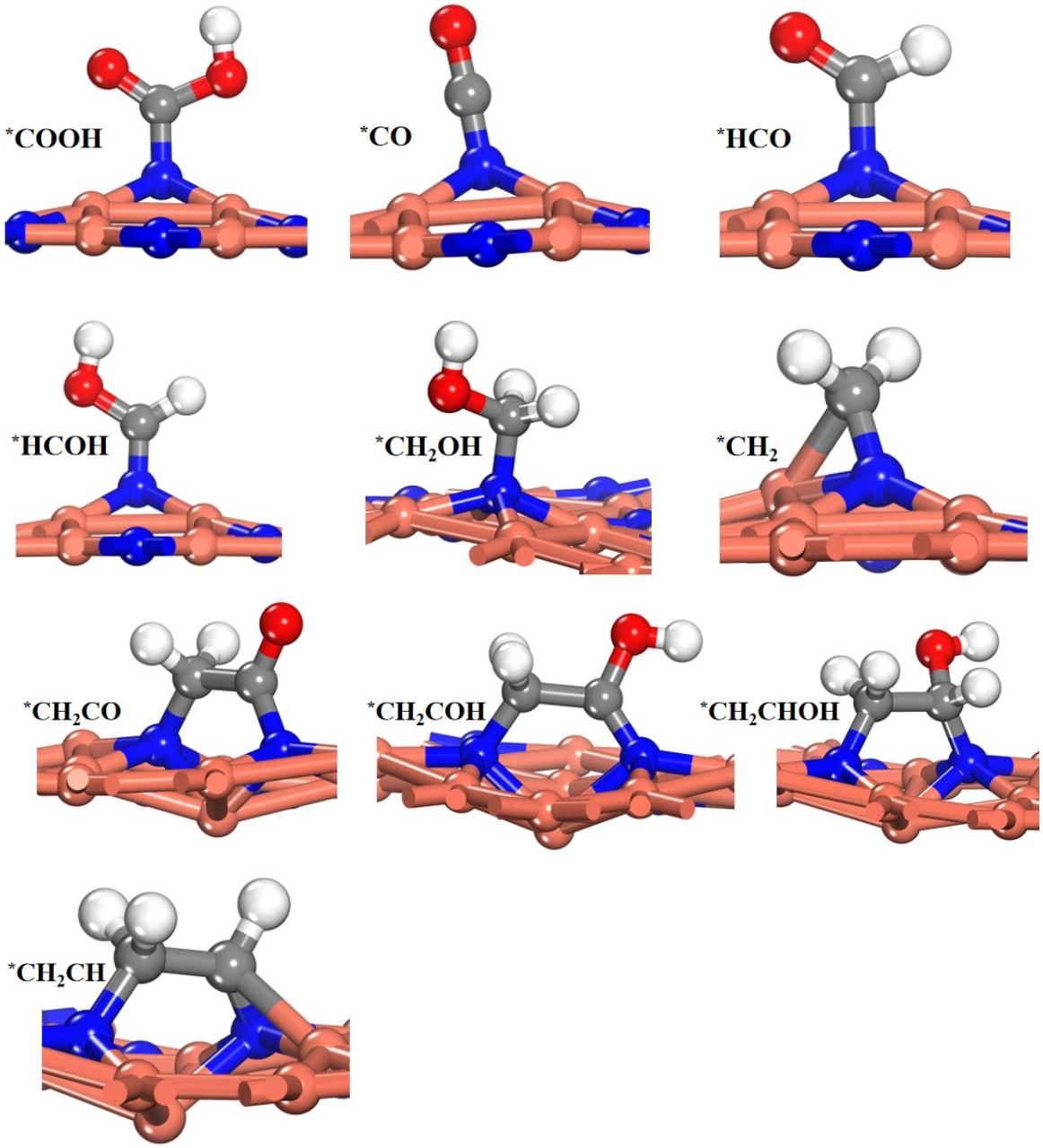

Fig. S5. The corresponding reaction intermediates of CO_2RR on Cu_2N monolayer along C_1 and C_2 pathways, where Cu, N, C, O, and H atoms are denoted by orange, blue, gray, red, and white balls, respectively.

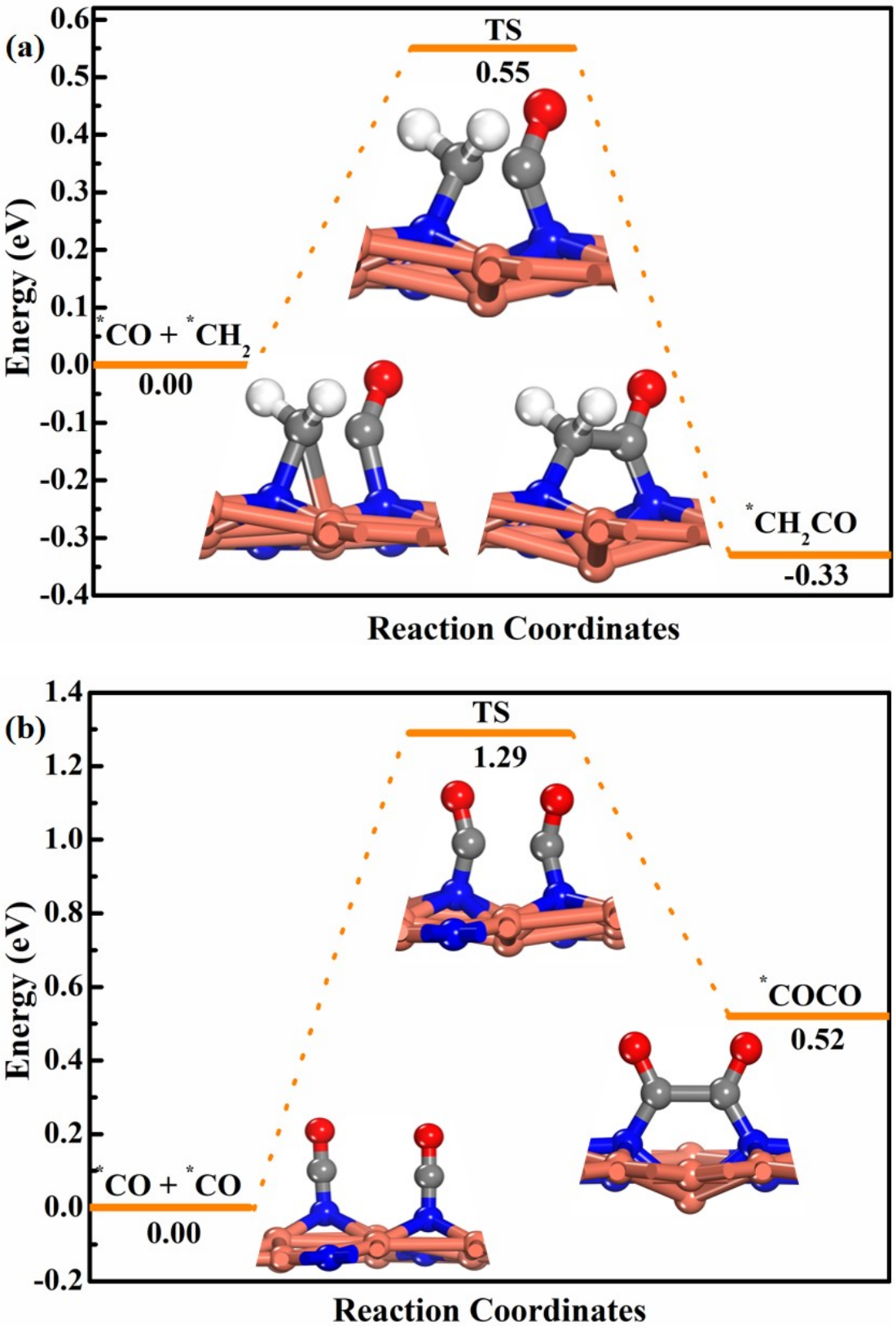

Fig. S6. The kinetic reaction pathway for C–C coupling along (a) carbene and (b) CO dimerization mechanisms. TS denotes the transition state.

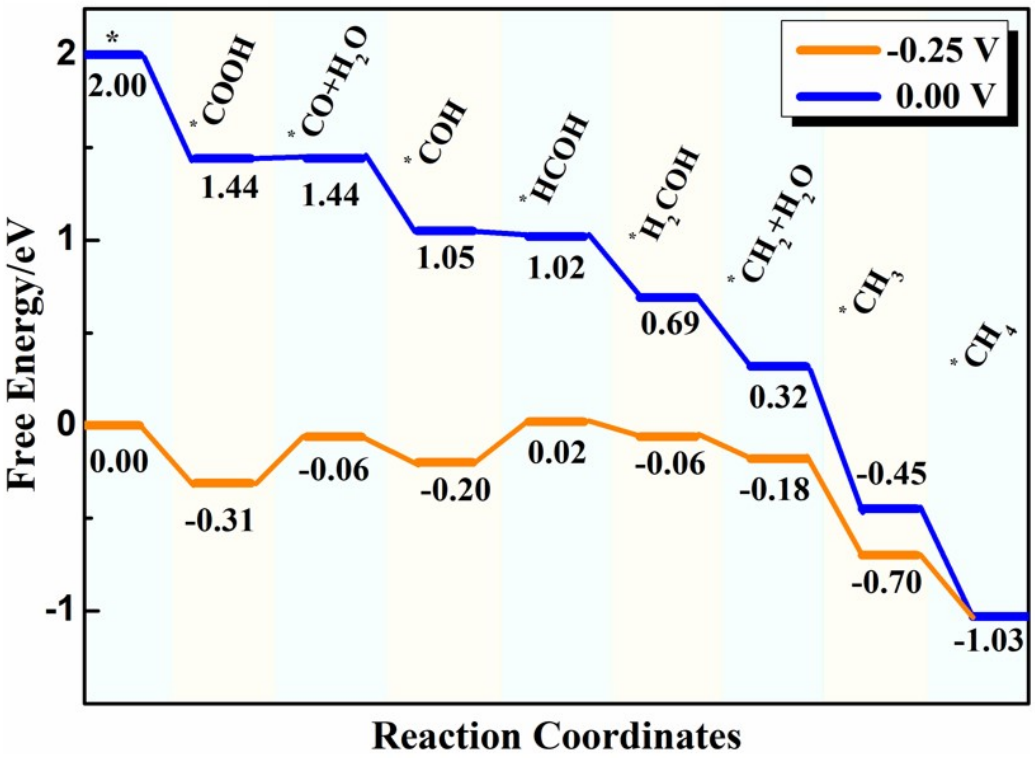

Fig. S7. The computed free energy profiles for the CO_2RR on Cu_2N monolayer along C_1 pathway with solvent effect.

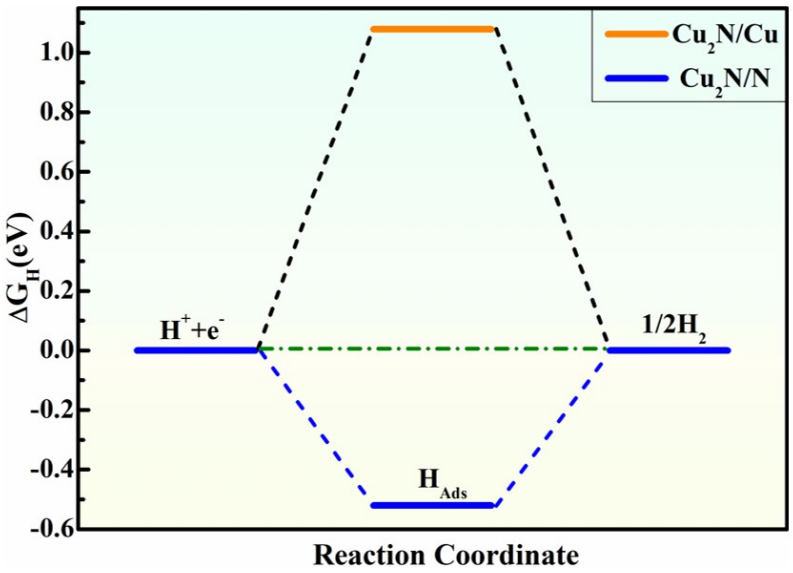

Fig. S8. The calculated Gibbs free profile of HER on various sites of Cu_2N monolayer.

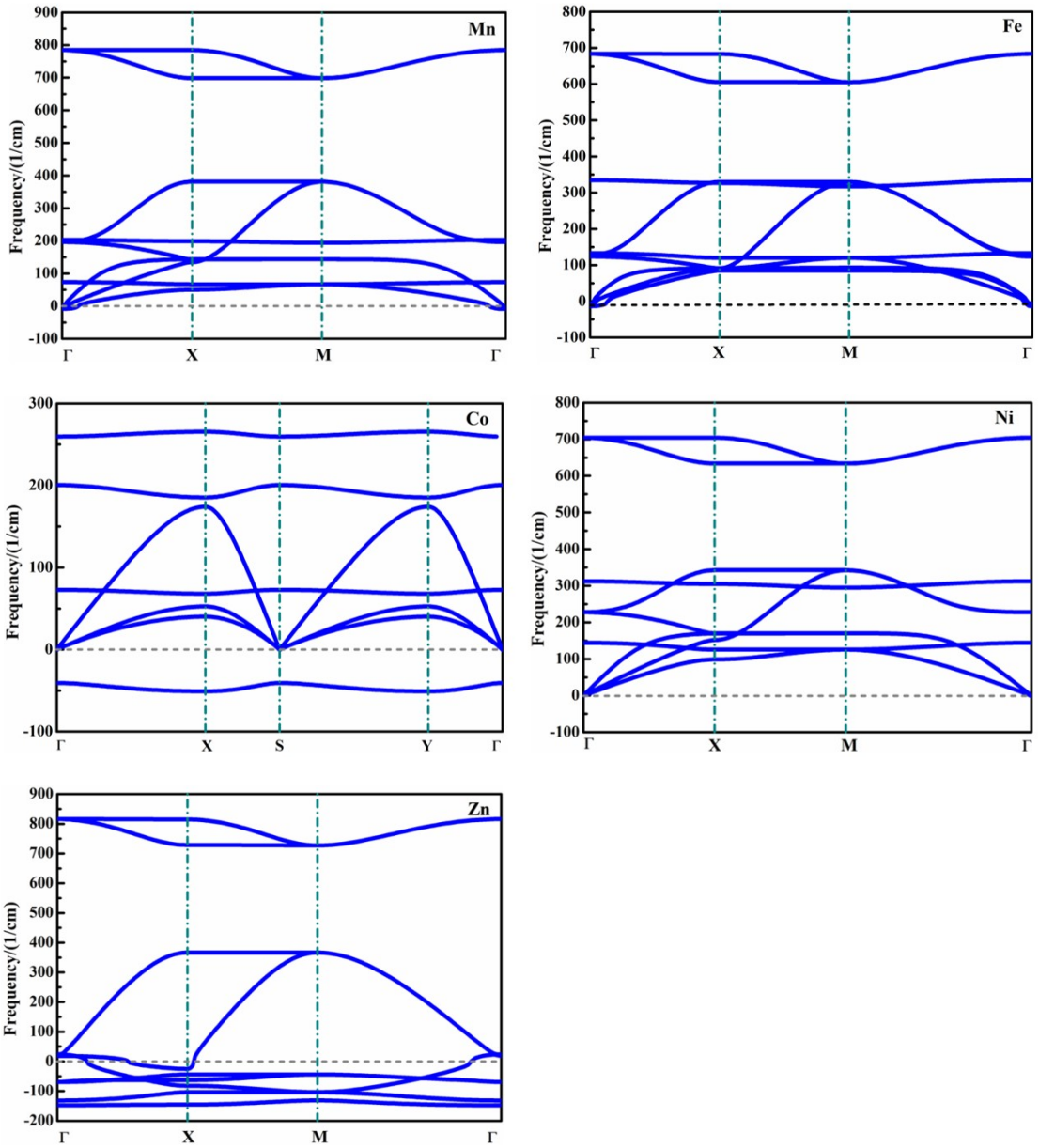

Fig. S9. The computed phonon dispersions of other predicted TM_2N (TM= Mn, Fe, Co, Ni, Zn) monolayers.

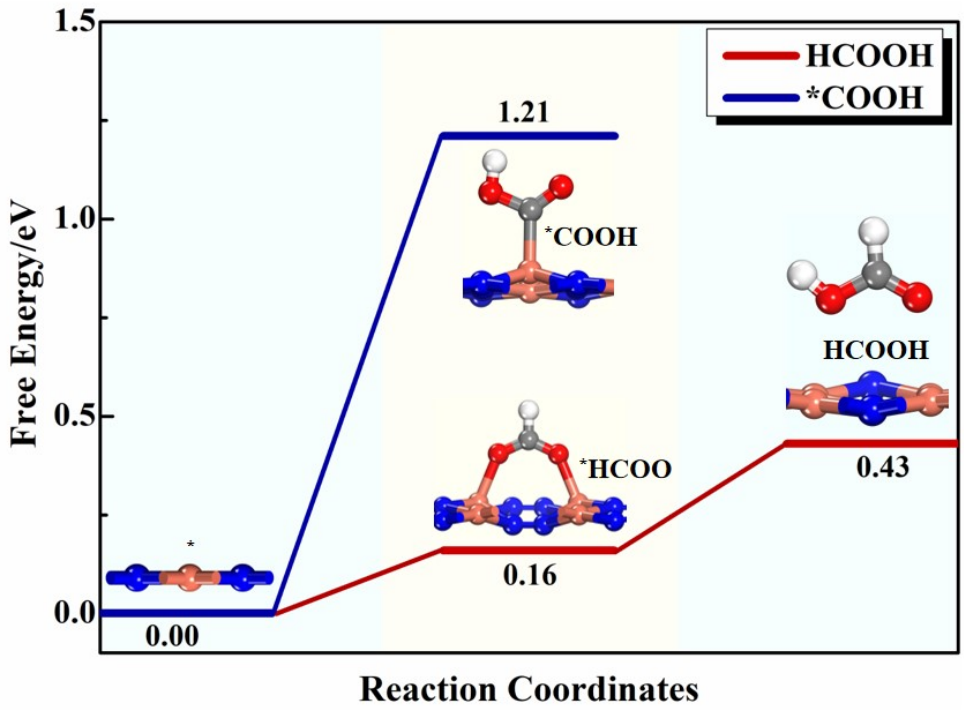

Fig. S10. The computed free energy profile and the corresponding intermediates for CO_2RR on CuN_2 monolayer.